Cell Tissue Res (2013) 352:551–559
DOI 10.1007/s00441-013-1604-z

REGULAR ARTICLE

Estrogen deficiency inhibits the odonto/osteogenic differentiation of dental pulp stem cells via activation of the NF-κB pathway

Yanping Wang · Ming Yan · Yan Yu · Jintao Wu · Jinhua Yu · Zhipeng Fan

Received: 10 December 2012 / Accepted: 1 March 2013 / Published online: 27 March 2013

Abstract Various factors can affect the functions of dental pulp stem cells (DPSCs). However, little knowledge is available about the effects of estrogen deficiency on the differentiation of DPSCs. In this study, an estrogen-deficient rat model was constructed and multi-colony-derived DPSCs were obtained from the incisors of ovariectomized (OVX) or sham-operated rats. Odonto/osteogenic differentiation and the possible involvement of the nuclear factor kappa B (NF-κB) pathway in the OVX-DPSCs/Sham-DPSCs of these rats were then investigated. OVX-DPSCs presented decreased odonto/osteogenic capacity and an activated NF-κB pathway, as compared with Sham-DPSCs. When the cellular NF-κB pathway was specifically inhibited by BMS345541, the odonto/osteogenic potential in OVX-DPSCs was significantly upregulated. Thus, estrogen deficiency down-regulated the odonto/osteogenic differentiation of DPSCs by activating NF-κB signaling and inhibition of the NF-κB pathway effectively rescued the decreased differentiation potential of DPSCs.

Keywords Dental pulp · Stem cell · Differentiation · Nuclear factor kappa B · Estrogen · Rat (Sprague Dawley, female)

Introduction

Dental pulp stem cells (DPSCs), a type of adult stem cell, have the potential of self-renewing and multi-differentiation and are considered as competent candidates for dental tissue regeneration, including bio-tooth reconstruction (Yan et al. 2011). Moreover, DPSCs are thought to be an ideal source of osteoblasts and mineralized tissues for bone regeneration, as they can co-differentiate into osteoblasts/endotheliocytes in vitro and form lamellar bone containing osteocytes in vivo (d'Aquino et al. 2007, 2009a, b; Graziano et al. 2008; Laino et al. 2005). To date, diverse studies have revealed that the biological features, especially the odonto/osteogenic capacity of DPSCs, can be affected by various conditions, such as the local microenvironment, cytokines, the age of the donor, in vitro passage number, morphogen and scaffold porogens (Demarco et al. 2010; Ma et al. 2009; Wang et al. 2011; Yang et al. 2012; Yu et al. 2010). However, little knowledge is available about the effects of estrogen on the differentiation of DPSCs.

Estrogen is an important hormone necessary for sex maturation and bone metabolism. Usually, estrogen deficiency brings about primary osteoporosis and bone fracture not only in post-menopausal women but also in elderly men (Khosla et al. 2011). Osteoporosis is thought to be the major cause of periodontal diseases, can lead to the loss of alveolar

This work was supported by the Medical Elitist Project of Jiangsu Province (no. RC2011140), National Natural Science Foundation of China (no. 81070798), Technology Support Program of Social Development of Jiangsu Province (no. BE2011778) and Priority Academic Program Development of Jiangsu Higher Education Institutions (PAPD, no. 2011-137)

The authors declare no conflicts of interest.

Y. Wang · M. Yan · Y. Yu · J. Wu · J. Yu
Institute of Stomatology, Nanjing Medical University,
140 Hanzhong Road, Nanjing,
Jiangsu 210029, People's Republic of China

J. Wu · J. Yu (✉)
Endodontic Department, School of Stomatology,
Nanjing Medical University, 136 Hanzhong Road, Nanjing,
Jiangsu 210029, People's Republic of China
e-mail: yuziyi_yjh@hotmail.com

J. Yu
e-mail: yuziyi_yjh@sohu.com

Z. Fan (✉)
Laboratory of Molecular Signaling and Stem Cells Therapy,
Molecular Laboratory for Gene Therapy and Tooth Regeneration,
Beijing Key Laboratory of Tooth Regeneration and Function Reconstruction, Capital Medical University School of Stomatology, 4 Tiantanxili,
Beijing 100050, People's Republic of China
e-mail: fanzhipengwang54384@hotmail.com

bone and can enhance the severity of periodontitis (Dvorak et al. 2009; Johnson et al. 1997; Mamalis et al. 2011; Moriya et al. 1998; Wattanaroonwong et al. 2011; Zhang et al. 2011a). Recent studies have revealed that estrogen can regulate the differentiation of periodontal ligament stem cells and bone marrow-derived mesenchymal stem cells (MSCs; Zhang et al. 2011a; Zhao et al. 2011). Estrogen deficiency suppresses osteogenic differentiation and the osteogenesis of MSCs but enhances their adipogenesis (Zhang et al. 2011a). When exposed to estrogen, these MSCs positively modulate alkaline phosphatase (ALP) activity and osteocalcin production (Cao et al. 2007; Kawamoto et al. 2002; Zhang et al. 2012), suggesting that estrogen has a positive effect on the osteogenic differentiation of MSCs. Whether estrogen deficiency can exert similar actions on DPSCs remains unknown.

In this study, we have established an estrogen-deficient rat model by bilateral ovariectomy (OVX) and investigated the role of estrogen in the odonto/osteogenic differentiation of DPSCs isolated from OVX-incisors (OVX-DPSCs). Our findings demonstrate that the odonto/osteogenic differentiation potential of OVX-DPSCs is significantly inhibited as compared with DPSCs from the sham-operated group (Sham-DPSCs) both in vitro and in vivo. Moreover, the blocking of the nuclear factor kappa B (NF-κB) pathway can rescue the decreased odonto/osteogenic capacity of OVX-DPSCs, indicating that estrogen regulates the differentiation of DPSCs via the intracellular NF-κB pathway.

Materials and methods

Establishment of an estrogen-deficient animal model

All animal experiments were conducted in accordance with the accepted standards of humane animal care and approved by the Animal Care Committee of Nanjing Medical University. The estrogen-deficient rat model was established as previously reported (Muhammad et al. 2012; Zhang et al. 2011a). Eight-week-old female Sprague Dawley (SD) rats from the Experimental Animal Center of Nanjing Medical University were randomly divided into two groups: the OVX group (OVX-rats; $n=15$) and sham-operated group (Sham-rats; $n=15$). All rats were anesthetized by 30 mg/ml pentobarbital, sterilized and both ovaries of OVX-rats were gently removed. Sham-operated rats were treated with the same incisions to expose the ovaries but without any damage to them. One month after the operation, the serum estradiol level was detected by immunochemiluminescent assay with the UniCel DxI 800 Immunoassay System (Beckman Coulter, USA). The body-weights of the rats at 0 month and 1 month post-operation were recorded. Data are presented as means ± SD.

Cell isolation and culture

One month after the operation, both OVX-rats and Sham-rats were killed by an overdose of pentobarbital. The lower incisors were carefully isolated and dental pulps were gently separated. Multi-colony derived Sham-DPSCs and OVX-DPSCs were obtained as previously described and cultured in alpha minimum essential medium (α-MEM; Gibco, USA) supplemented with 10% fetal bovine serum (FBS; Hyclone, USA), 100 U/ml penicillin and 100 μg/ml streptomycin at 37°C under 5% CO_2. The culture medium was changed every 3 days and the cells were routinely observed under a phase-contrast inverted microscope (Olympus, Germany). Sham-DPSCs or OVX-DPSCs at passage 2–3 were used in the following experiments.

MTT assay

DPSCs were seeded into 96-well plates (Nunc, USA) at a density of 2×10^3 cells/well for 24 h and starved in a serum-free medium for another 24 h. The serum-free medium was then replaced with the routine medium. For nine consecutive days, fresh MTT (3-[4, 5-dimethylthiazol-2-yl]-2,5-diphenyl-2,5-tetrazoliumbromide) solution (5 mg/ml; Sigma-Aldrich, USA) was added to the wells, which were then incubated for 4 h at 37°C. The MTT solution was removed, formazan was solubilized in 150 μl/well dimethyl sulfoxide (DMSO, Sigma-Aldrich, USA) and the absorbance (OD value) was measured at 490 nm by using a microtiter plate reader (Titertek, Finland). The experiment was repeated three times and data are presented as means ± SD.

Flow cytometry

DPSCs were seeded into 6-cm culture dishes (Nunc, USA) in routine culture media supplemented with 10% FBS for 24 h. After 24 h of starvation with serum-free medium, the medium containing 10% FBS was added back to the cultures and changed every 3 days until 70%–75% confluence. The cells were then harvested and fixed with 75% ice-cold ethanol at 4°C for 30 min in the dark. DNA content was measured by a FAC Scan flow cytometer (BD Biosciences, USA). Cell cycle fractions (G_0, G_1, S, and G_2M phases) were determined by flow cytometry. The experiment was repeated in triplicate.

ALP activity assay and Alizarin red staining

DPSCs were seeded into 96-well plates (Nunc, USA) at a density of 2×10^3 cells/well and cultured in routine medium or mineralization-inducing medium (MM) containing α-MEM, 10% fetal bovine serum, 100 U/ml penicillin, 100 μg/ml streptomycin, 100 μM ascorbic acid, 2 mM 2-glycerophosphate and 10 nM dexamethasone. The ALP

activity assay was performed as previously reported (Wang et al. 2012) by using an ALP activity kit (Sigma-Aldrich, USA) and normalized to total protein content in the cell. Alizarin red staining was performed at day 14 as previously described (Yu et al. 2010). The staining of calcified nodules was eluted by using 10% cetylpyridinium chloride (CPC) in 10 mM sodium phosphate (pH7.0). The calcium concentration was determined by measuring the absorbance at 526 nm with a universal microplate reader (BioTek Instruments, USA). This experiment was performed in triplicate and the results are presented as means ± SD.

Real-time reverse transcription plus the polymerase chain reaction

Total cellular RNA of DPSCs was obtained by adding TRIzol reagent (Invitrogen, USA) to cell samples following the manufacturer's instructions. The mRNA was reverse-transcribed into cDNA by using a PrimeScript RT Master Mix kit (TaKaRa Biotechnology, China). Real-time reverse transcription plus the polymerase chain reaction (RT-PCR) was performed by using the SYBR Premix Ex Taq kit (TaKaRa Bio, Japan) and ABI 7300 real-time PCR system. Primers used in this experiment are listed in Table 1. *D-gluteraldehyde-3-phosphate dehydrogenase* (*Gapdh*) was used as an internal control. The expression of genes was calculated by the method of $2^{-\Delta\Delta Ct}$ as previously reported (Wang et al. 2012). Data are shown as means ± SD of three independent experiments.

Western blot analysis

DPSCs were washed twice with 0.01 M phosphate-buffered saline (PBS) and lysed in RIPA lysis buffer (Beyotime, China) containing 1 mM phenylmethane sulfonyl-fluoride according to the manufacturer's instructions. The protein concentration was measured via Bradford protein assay. Protein (30 μg) was loaded onto a 10% SDS-polyacrylamide gel for electrophoresis and then transferred onto 0.22 μm polyvinylidene difluoride membranes (Millipore, Bedford, Mass., USA) at 300 mA for 1 h in a blotting apparatus (Bio-Rad, USA). Membranes were blocked in the blocking solution (5% non-fat dried skimmed milk powder, 0.01 M PBS, 0.1% Tween-20) at room temperature for 2 h and incubated in primary antibodies (RUNX2, 1:1000, Abcam; OSX, 1:1000, Abcam; OCN, 1:1000, Abcam; DSP, 1:500, Santa Cruz; β-ACTIN, 1:1000, Bioworld) overnight at 4°C. Finally, the membranes were washed three times with PBS with Tween for 10 min followed by incubation in the relevant secondary antibodies (1:10000, Boster, China) for 1 h at 37°C, visualized by SuperSignal West Pico Chemiluminescent Substrate (Thermo, USA) and exposed to Kodak X-ray films. β-ACTIN served as an internal control.

In vivo transplantation

DPSCs (1×10^6) were collected as cell pellets by exposure to 0.25% trypsin/EDTA for 3 min and centrifugation at 1000 rpm for 5 min in a sterile tube and seeded gently onto absorbable gelatin sponges (AGS, Nanjing Pharmaceuticals, China), which served as carriers as previously described (Wang et al. 2012; Yu et al. 2012). Then, the cell pellets were transplanted into the renal capsules of adult female SD rats. After 14 days of in vivo culture, the retrieved implants ($n=10$) were fixed in 4% polyoxymethylene for 48 h, decalcified with 10% EDTA (pH8.0) and embedded in paraffin. Finally, paraffin sections (5 μm) were processed for hematoxylin and eosin (HE) staining.

Immunohistochemical staining

Immunohistochemical analyses were performed by using the streptavidin-biotin complex method according to the manufacturer's recommended protocols. Briefly, tissue sections

Table 1 Sense and antisense primers for real-time reverse transcription plus the polymerase chain reaction (*F* forward, *R* reverse, *Alp* alkaline phosphatase, *Runx2* Runt-related transcription factor 2, *Osx* osterix, *Ocn* osteocalcin, *Dspp* dentin sialophosphoprotein, *Gapdh* D-gluteraldehyde-3-phosphate dehydrogenase)

Genes	GeneBank number	Sequences (5′-3′)	Length of product
Alp	NM_013059.1	F: CGAGCAGGAACAGAAGTTTGC R: GAATCCGACCCACGGAGG	64 bp
Runx2	NM_053470.2	F: AATGCCTCCGCTGTTATG R: TTCTGTCTGTGCCTTCTTG	191 bp
Osx	NM_001037632.1	F: GCCTACTTACCCGTCTGACTTT R: GCCCACTATTGCCAACTGC	131 bp
Ocn	NM_013414.1	F: AAGCCCAGCGACTCTGAGTCT R: CCGGAGTCTATTCACCACCTTACT	75 bp
Dspp	NM_012790.2	F: CGTTCAGGGAGTCCTAGCGGGAACG R: GTGACTCTCCCTTCCATCTCCTG	99 bp
Gapdh	NM_017008.4	F: GCCTCGTCTCATAGACAAGATGGT R: GAAGGCAGCCCTGGTAACC	82 bp

from representative paraffin blocks were deparaffinized in xylene and rehydrated through graded ethanol solutions. Endogenous peroxidases were blocked by using 3% hydrogen peroxide. For antigen retrieval, the sections were processed by conventional microwave heating in 0.01 M sodium citrate retrieval buffer (0.01 M sodium citrate, 0.01 M citric acid, pH6.0) for 5 min. Then, the sections were blocked by 10% normal swine serum for 20 min and incubated with primary antibodies (DSP, 1:200; OCN, 1:100) overnight at 4°C. Incubation with PBS instead of primary antibodies served as the negative control. Finally, the sections were incubated with the relevant secondary antibodies for 45 min at room temperature. The reaction products were developed in 3, 3′-diaminobenzidine solution with hydrogen peroxide and counterstained with hematoxylin.

Enzyme-linked immunosorbent assay

To determine the tumor necrosis factor-α (TNF-α) concentration, 1 ml culture supernatant of DPSCs grown in 25 mm^2 flasks was collected after 5 days of culture in routine medium. Then, the medium was centrifugated at 3000 rpm to exclude solid substances. Enzyme-linked immunosorbent assay (ELISA) was performed by using a rat TNF-α ELISA kit (EX Cell Biology, China). The experiment was repeated three times.

Statistics

For independent samples, the two-tailed *t*-test was performed with SPSS 13.0 software. *P*-values less than 0.05 were considered statistically significant.

Results

Estrogen deficiency had no effect on the proliferation of DPSCs

One month after ovariectomy, the serum estradiol in OVX-rats was significantly declined (Fig. 1a), whereas the body weight of OVX-rats was heavier than that of Sham-rats (Fig. 1b), indicating that the estrogen-deficient rat model had successfully been established.

OVX-DPSCs and Sham-DPSCs were then respectively isolated from OVX and Sham-operated rat incisors, which shared almost the same appearance at the 2nd passage (Fig. 1c, d). No significant difference of proliferation index (PI = S + G_2M) was observed between Sham-DPSCs and OVX-DPSCs (Fig. 2a–c). The MTT assay further demonstrated that the cell proliferation of these two types of DPSCs was similar (Fig. 2d).

Estrogen deficiency inhibited the odonto/osteogenic differentiation potential of DPSCs

First, we detected the early-stage marker of odonto/osteogenic differentiation, i.e., ALP activity in OVX-DPSCs or Sham-DPSCs. The results showed that ALP activity in Sham-DPSCs at day 3 was significantly higher than that in OVX-DPSCs irrespective of whether the cells were grown in the routine culture medium or mineralization-inducing medium (Fig. 3a). Moreover, Alizarin red staining and quantitative calcium measurement demonstrated that the Sham-DPSC group generated more calcium nodules than the OVX-DPSC

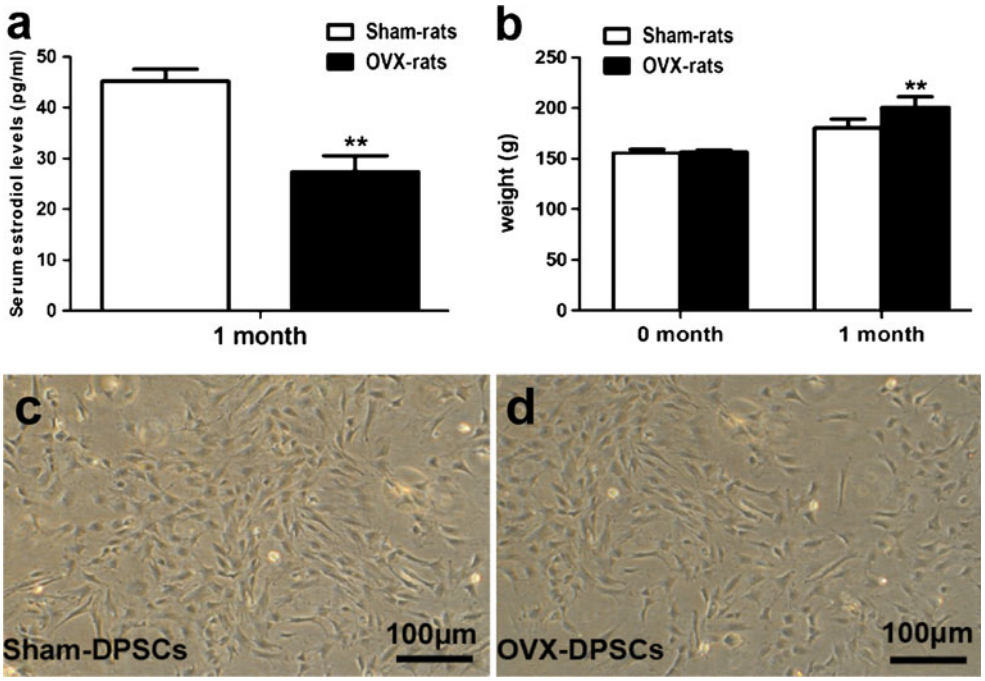

Fig. 1 Establishment of an animal model for estrogen deficiency and isolation of dental pulp stem cells. **a** Serum estradiol was detected by the immunochemiluminescent assay. Levels of serum estradiol in ovariectomized rats (*OVX-rats*) were significantly lower than those of the sham-operated rat group (*Sham-rats*) at one month after operation. **b** Body-weight evaluation showed that OVX-rats were significantly heavier than Sham-rats at one month after operation. $^{**}P<0.01$; values were means ± SD, $n=15$. **c**, **d** Multi-colony-derived dental pulp stem cells from Sham-rats (*Sham-DPSCs*) and from OVX-rats (*OVX-DPSCs*) had similar morphological features. *Bars* 100 μm

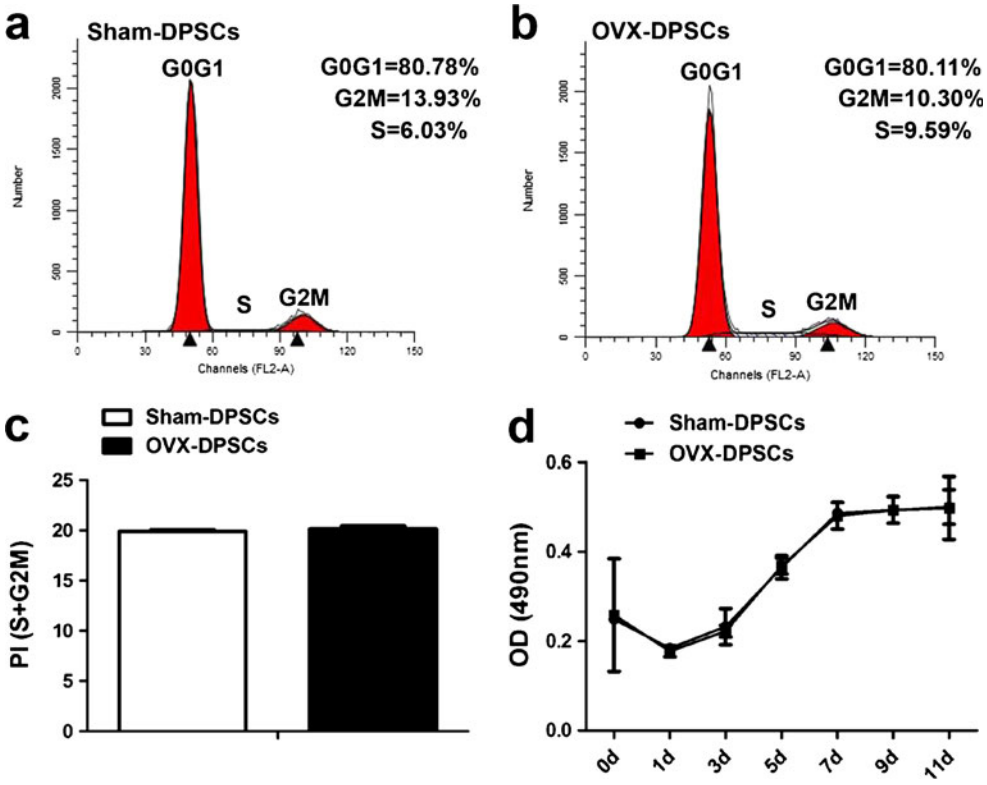

Fig. 2 Comparison of cell proliferation between Sham-DPSCs and OVX-DPSCs.**a** Average proliferation index (PI = S + G2M) in Sham-DPSCs is 19.96% by flow cytometry (FCM) assay. **b** Average PI in OVX-DPSCs is 19.89% by FCM assay. **c** No significant difference of average PI is seen between the OVX and Sham groups. Values are means ± SD, n=3. **d** MTT assay shows no significant difference of growth curves between Sham-DPSCs and OVX-DPSCs (*OD* optical density, *d* days). Values are means ± SD, n=6

group after 14 days of osteogenic induction (Fig. 3b, c). Real-time RT-PCR results demonstrated that the mRNA levels of odonto/osteogenic markers, namely (*Alp* (alkaline phosphatase), *Runx2* (Runt-related transcription factor 2), *Osx*

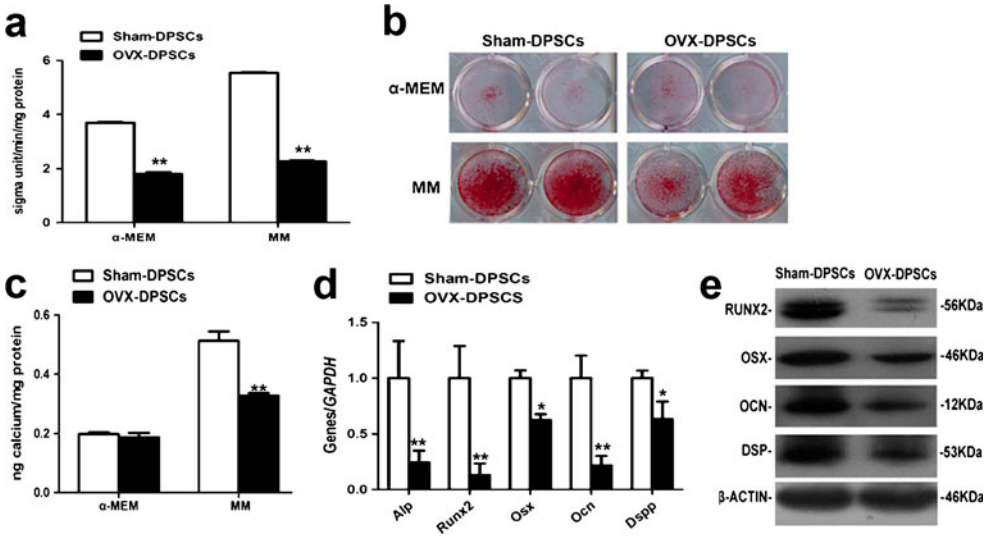

Fig. 3 In vitro odonto/osteogenic differentiation capacity in OVX-DPSCs and Sham-DPSCs.**a** Alkaline phosphatase (ALP) activity in OVX-DPSCs is significantly lower than that in Sham-DPSCs, respectively, in routine medium (*α-MEM*) and mineralization-inducing medium (*MM*) at day 3. **P<0.01. Values are means ± SD, n=6. **b**, **c** Alizarin red staining and quantitative calcium measurement show that OVX-DPSCs form fewer calcified nodules than Sham-DPSCs at day 14 in mineralization-inducing medium. **P<0.01. Values are means ± SD, n=6. **d** Results from real-time reverse transcription plus the polymerase chain reaction (RT-PCR) show that the gene expression of *Alp* (alkaline phosphatase), *Runx2* (Runt-related transcription factor 2), *Osx* (osterix), *Ocn* (osteocalcin) and *Dspp* (dentin sialophosphoprotein) in OVX-DPSCs is significantly lower than that in Sham-DPSCs at day 7 in mineralization-inducing medium. *GAPDH* (D-gluteraldehyde-3-phosphate dehydrogenase) served as an internal control. Values are means ± SD. **$2^{-\Delta\Delta Ct}\geq 2$, P<0.01; *$1<2^{-\Delta\Delta Ct}<2$, P<0.01. **e** Western blot results clearly show that the protein levels of RUNX2, OSX, OCN, and DSP are down-regulated more in OVX-DPSCs than in Sham-DPSCs at day 7 in mineralization-inducing medium. β-ACTIN served as an internal control

(osterix), *Ocn* (osteocalcin) and *Dspp* (dentin sialophosphoprotein) were increased in Sham-DPSCs as compared with OVX-DPSCs after 7 days of osteogenic induction (Fig. 3d). Western blot also revealed that the protein expression of RUNX2, OSX, OCN and DSP was enhanced in Sham-DPSCs in comparison with OVX-DPSCs at day 7 in mineralization-inducing medium ($P<0.01$; Fig. 3e).

Furthermore, we investigated the odonto/osteogenesis of OVX-DPSCs and Sham-DPSCs in vivo. The implants were harvested 2 weeks post-transplantation for HE and immunohistochemical staining. HE staining showed that both Sham-DPSCs and OVX-DPSCs could form dentin-pulp-like and osteodentin-like tissues in vivo. However, the dentin-pulp complex generated by Sham-DPSCs (Fig. 4e–g) was more regular and typical than that of the OVX-DPSC group (Fig. 4m–o). Immunohistochemical staining demonstrated that the expression of DSP and OCN in osteodentin structures was stronger in the Sham-DPSC group (Fig. 4b, c) than that in the OVX-DPSC group (Fig. 4j, k). In addition, the expression of DSP in dentin tissues was stronger in the Sham-DPSC group (Fig. 4f) than that in the OVX-DPSC group (Fig. 4n).

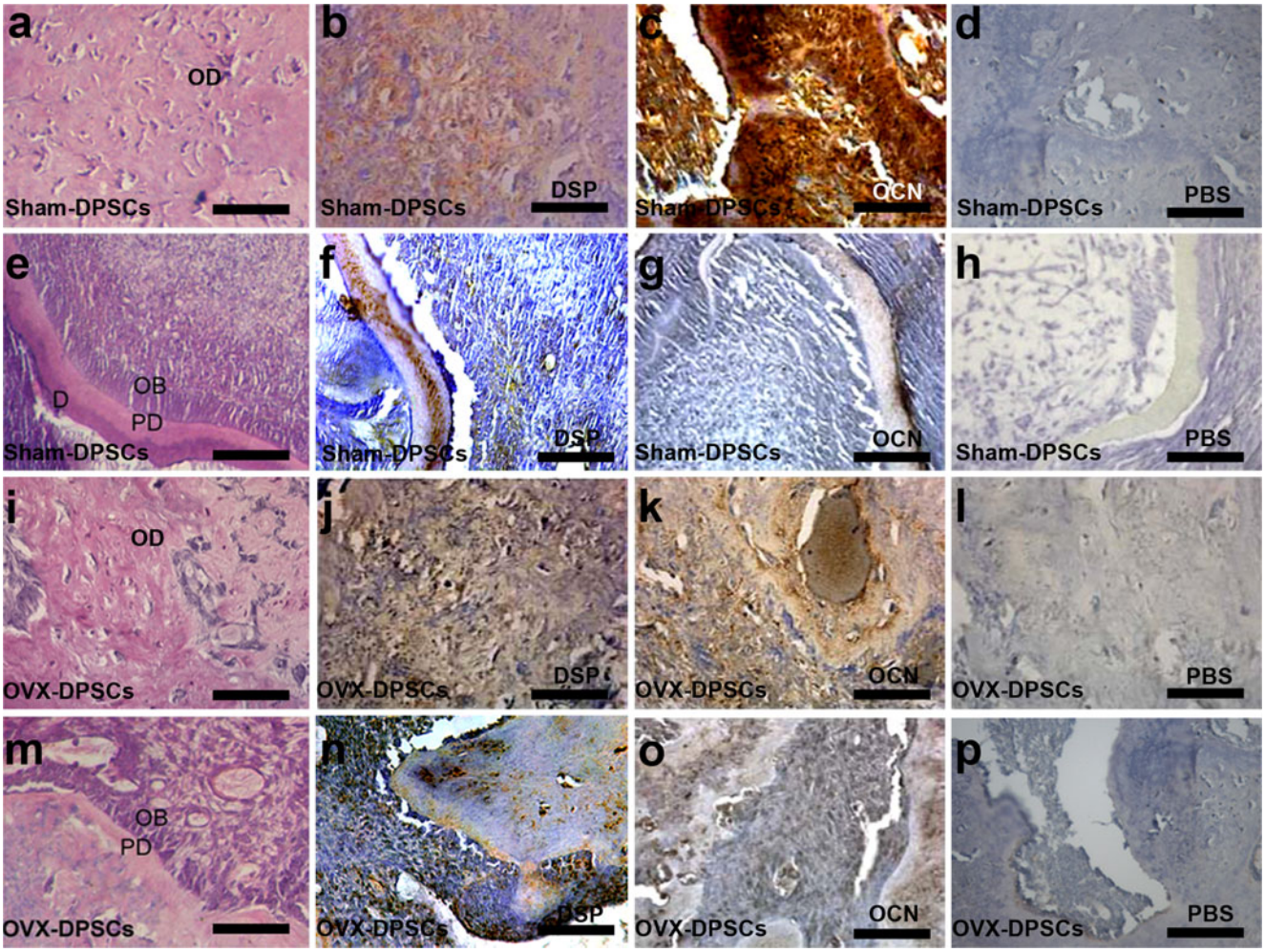

Fig. 4 In vivo odonto/osteogenesis of OVX-DPSCs and Sham-DPSCs.**a-d** Osteodentin-like tissues were formed in the Sham-DPSC group. HE staining (**a**) showed osteodentin-like (*OD*) structures with osteocyte-like cells embedded in the matrix lacunae. Immunohistochemical results demonstrated positive staining for dentin sialophosphoprotein (*DSP*, **b**) and strong positive staining for osteocalcin (*OCN*, **c**) in osteodentin-like structures in the Sham-DPSCs group. Phosphate-buffered saline (*PBS*) instead of primary antibodies served as a negative control (**d**). **e-h** Typical dentin pulp complexes were generated in Sham-DPSCs implants. HE staining demonstrated dentin-pulp-like structures in the Sham group (**e**) containing predentin (*PD*), mature dentin (*D*) and the odontoblastic layer (*OB*). Immunohistochemical findings showed strong staining for DSP (**f**) and negative staining for OCN in dentin and pulp regions (**g**). PBS instead of primary antibodies served as a negative control (**h**). **i-l** Osteodentin-like tissues were generated in OVX-DPSC implants. HE staining showed osteodentin-like structures containing osteocyte-like cells and matrix lacunae (**i**). Weak staining for DSP (**j**) and OCN (**k**) was detected in the osteodentin-like matrix. PBS instead of primary antibodies was used as a negative control (**l**). **m-p** Typical dentin-pulp-like tissues were formed in the OVX-DPSC group. HE staining showed atypical dentin-pulp-like structures (**m**) containing predentin (*PD*) and odontoblast-like cells (*OB*). Weak staining for DSP (**n**) and almost no staining for OCN (**o**) were apparent in the dentin-pulp structures. PBS instead of primary antibodies served as a negative control (**p**). *Bars* 100 μm

NF-κB pathway plays a key role in regulating the odonto/osteogenic differentiation of OVX-DPSCs

ELISA results showed that TNF-α (the putative activator of the canonical NF-κB pathway) levels in the culture supernatant of OVX-DPSCs were significantly higher than those of Sham-DPSCs (Fig. 5a). Western blot further revealed that the expression of cytoplasmic phosphorylated IκBα, P65, phosphorylated P65 and nuclear P65 were obviously up-regulated in OVX-DPSCs as compared with the counterparts in Sham-DPSCs (Fig. 5b). These data indicated an active NF-κB pathway in OVX-DPSCs. When OVX-DPSCs were treated with BMS345541 (an NF-κB pathway inhibitor), the odonto/osteogenic genes (*Alp*, *Osx*, *Runx2*, *Ocn* and *Dspp*) in OVX-DPSCs were strikingly up-regulated (Fig. 5d). Similarly, the protein levels of ALP, RUNX2, OSX, OCN and DSP were also increased after BMS345541 treatment of OVX-DPSCs (Fig. 5c, e).

Discussion

To date, a large number of research studies have investigated the effects of estrogen deficiency on bone and on bone-marrow-derived MSCs and have demonstrated the negative modulation of estrogen deficiency on the osteogenesis and osteogenic differentiation of bone-marrow-derived MSCs. In this study, we have elucidated, for the first time, that estrogen deficiency can affect the differentiation of DPSCs, i.e., estrogen deficiency in OVX rats down-regulates the odonto/osteogenic capability of DPSCs, as indicated by their low ALP activity, decreased mineralization, reduced expression of odonto/osteoblast markers (*Alp*, *Runx2*/RUNX2, *Osx*/OSX, *Ocn*/OCN and *Dspp*/DSP) in vitro and weakened dentino/osteogenesis in vivo in OVX-DPSCs as compared with Sham-DPSCs.

As the major markers of odontoblast differentiation, DSP protein and *Dspp* mRNA have been reported to be present mostly in secretory odontoblasts (Chen et al. 2009; Iejima et al. 2007). The decreased expression of DSP/*Dspp* in the OVX group indicates that estrogen deficiency delays the odontoblastic differentiation of DPSCs in vitro. Transplantation results have further demonstrated that Sham-DPSCs can form a regular dentin-pulp complex, whereas OVX-DPSCs only generate irregular dentin-pulp structures with reduced DSP expression, indicating that estrogen deficiency can weaken the dentinogenic capacity of DPSCs in vivo. Thus, we can reasonably suggest that the regenerative capacity of the dental-pulp complex in patients with estrogen deficiency might be affected because of the decreased dentinogenic potency of the DPSCs in their dental pulp tissues.

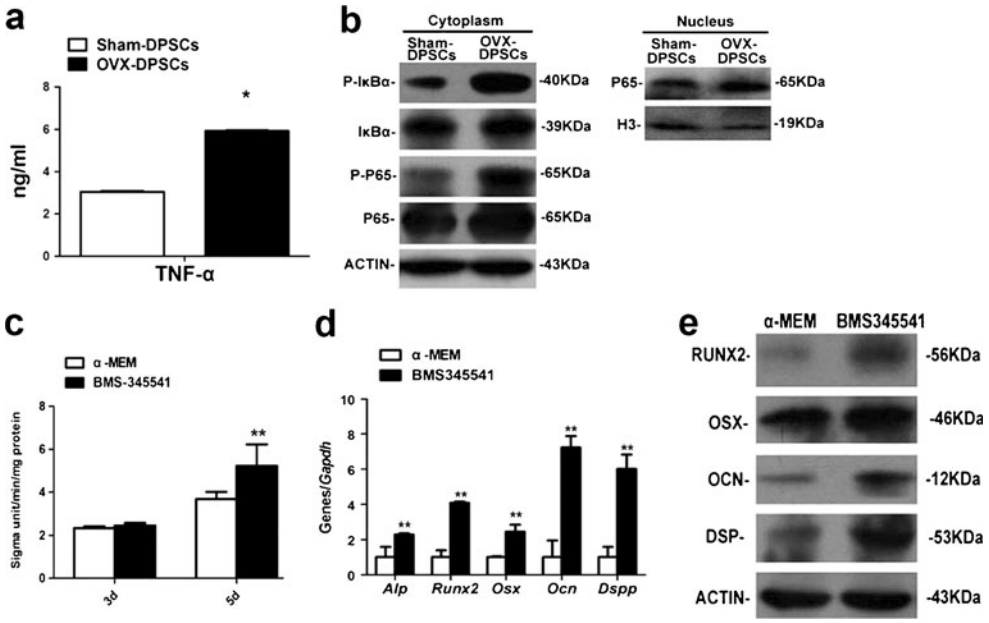

Fig. 5 Nuclear factor kappa B (NF-κB) pathway involvement in the odonto/osteogenic differentiation of OVX-DPSCs.**a** Tumor necrosis factor-α (*TNF-α*) in the supernatants of Sham-DPSCs and OVX-DPSCs was detected by enzyme-linked immunosorbent assay. The TNF-α concentration in the OVX-DPSC group was significantly higher than that in the Sham-DPSC group. **P*<0.05, *n*=3. **b** Western blot results demonstrated the protein levels of cytoplasmic P-IκBα, IκBα, P65 and P-P65 and nuclear P65 in Sham-DPSCs and in OVX-DPSCs. Cytoplasmic P-IκBα, P65 and P-P65 and nuclear P65 were highly expressed in OVX-DPSCs as compared with Sham-DPSCs. β-ACTIN (*ACTIN*) and Histone H3 (*H3*) served as an internal control, respectively, in cytoplasm and nucleus. *c* ALP activity was increased in BMS345541 treated OVX-DPSCs, as compared with the untreated counterparts (*d* days). **d** When treated with the NF-κB inhibitor (1 μM BMS345541), real-time RT-PCR results showed that the gene expression of Alp, Runx2, Ocn and Dspp was significantly up-regulated in OVX-DPSCs . **$2^{-\Delta\Delta Ct} \geq 2$, *P*<0.01, *n*=3. **e** Protein levels of RUNX2, OSX, OCN and DSP were higher in BMS345541-treated OVX-DPSCs than in untreated OVX-DPSCs

RUNX2, OSX and OCN are commonly believed to play an important role in osteogenesis (Chen et al. 2009; Ni et al. 2011). Both RUNX2 and OSX are early-stage markers of osteoblastic differentiation (Komori 2010; Ni et al. 2011; Wade-Gueye et al. 2012). *Runx2* overexpression can induce MSCs to differentiate along the osteoblast lineages, enhance new bone formation and even drive preadipocytes into bone-forming cells in vitro (Takahashi 2011; Zhang et al. 2011b). *Osx* is the downstream gene of the BMP-2/Smad/Runx2 signaling pathway and is highly expressed in functional odonto/osteoblasts (Celil et al. 2005). The decrease of RUNX2/OSX expression in OVX-DPSCs implies a weakened matrix mineralization and differentiation ability towards the osteoblast lineages. OCN is mainly expressed in the late stages of osteoblastic differentiation (Ni et al. 2011; Wang et al. 2012). As compared with Sham-DPSCs implants, OCN protein expression in osteodentin structures is decreased in OVX-DPSC implants, indicating that estrogen deficiency can suppress the osteogenic capacity of DPSCs in vivo. Taken together, the low-level expression of RUNX2/OSX/OCN in OVX-DPSCs suggests that the osteogenic capacity of OVX-DPSCs is down-regulated not only in the early stages of osteoblastic differentiation but also in the late stages of matrix mineralization.

Various studies have established that estrogen can inhibit the NF-κB pathway in many physiological and pathological processes (Fahey et al. 2008; Giannoni et al. 2011; Kanda and Watanabe 2003). In this study, we have determined that the NF-κB pathway is involved in odonto/osteogenic differentiation of OVX-DPSCs. The highly expressed TNF-α cytokine and NF-κB-related proteins in the OVX-DPSC group indicate that the intracellular NF-κB pathway is activated in OVX-DPSCs. In other words, the absence of estrogen liberates the inhibition of the NF-κB pathway. Activation of the NF-κB signaling pathway plays a pivotal role in the negative modulation of osteoblastic differentiation and mineralization (Tang et al. 2013), whereas suppression of NF-κB can enhance bone formation and ameliorate osteopenia in ovariectomized mice (Alles et al. 2010; Yamaguchi et al. 2011). The present findings have revealed that the blocking of the NF-κB pathway by BMS345541 can rescue the decreased odonto/osteogenic competence of OVX-DPSCs, indicating that the differentiation of DPSCs is negatively modulated by the NF-κB pathway. Since the activation of the cellular NF-κB pathway can diminish osteogenic differentiation (Franke et al. 2011; Lee et al. 2012; Xu et al. 2009), estrogen deficiency might inhibit the odonto/osteogenic capacity of DPSCs by activating the NF-κB pathway. BMS345541 can take the place of estrogen to inhibit the activity of the NF-κB pathway in OVX-DPSCs and ultimately restore their down-regulated odonto/osteogenic differentiation potential. However, more studies are required to investigate other mechanisms embedded in the reduced odonto/osteogenic differentiation of OVX-DPSCs.

In conclusion, estrogen deficiency down-regulates the odonto/osteogenic potential of DPSCs via the NF-κB pathway and inhibition of the NF-κB signaling pathway can significantly improve the reduced odonto/osteogenic potential of OVX-DPSCs. BMS34554 can be used as an effective reagent to rescue the decreased differentiation potential of OVX-DPSCs. Therefore, the use of DPSCs from donors with estrogen deficiency in future tooth/bone regeneration might not be a good idea, unless these stem cells are modified in vitro.

Acknowledgments The authors thank Dr. Ruoning Wang for his help in improving the language in this manuscript.

References

Alles N, Soysa NS, Hayashi J, Khan M, Shimoda A, Shimokawa H, Ritzeler O, Akiyoshi K, Aoki K, Ohya K (2010) Suppression of NF-kappaB increases bone formation and ameliorates osteopenia in ovariectomized mice. Endocrinology 151:4626–4634

Cao M, Shu L, Li J, Su J, Zhang W, Wang Q, Guo T, Ding Y (2007) The expression of estrogen receptors and the effects of estrogen on human periodontal ligament cells. Methods Find Exp Clin Pharmacol 29:329–335

Celil AB, Hollinger JO, Campbell PG (2005) Osx transcriptional regulation is mediated by additional pathways to BMP2/Smad signaling. J Cell Biochem 95:518–528

Chen S, Gluhak-Heinrich J, Wang YH, Wu YM, Chuang HH, Chen L, Yuan GH, Dong J, Gay I, MacDougall M (2009) Runx2, osx, and dspp in tooth development. J Dent Res 88:904–909

d'Aquino R, Graziano A, Sampaolesi M, Laino G, Pirozzi G, De Rosa A, Papaccio G (2007) Human postnatal dental pulp cells co-differentiate into osteoblasts and endotheliocytes: a pivotal synergy leading to adult bone tissue formation. Cell Death Differ 14:1162–1171

d'Aquino R, De Rosa A, Laino G, Caruso F, Guida L, Rullo R, Checchi V, Laino L, Tirino V, Papaccio G (2009a) Human dental pulp stem cells: from biology to clinical applications. J Exp Zool B Mol Dev Evol 312B:408–415

d'Aquino R, De Rosa A, Lanza V, Tirino V, Laino L, Graziano A, Desiderio V, Laino G, Papaccio G (2009b) Human mandible bone defect repair by the grafting of dental pulp stem/progenitor cells and collagen sponge biocomplexes. Eur Cell Mater 18:75–83

Demarco FF, Casagrande L, Zhang Z, Dong Z, Tarquinio SB, Zeitlin BD, Shi S, Smith AJ, Nor JE (2010) Effects of morphogen and scaffold porogen on the differentiation of dental pulp stem cells. J Endod 36:1805–1811

Dvorak G, Reich K, Tangl S, Lill CA, Gottschalk-Baron M, Watzek G, Gruber R, Haas R (2009) Periodontal histomorphometry and status of aged sheep subjected to ovariectomy, malnutrition and glucocorticoid application. Arch Oral Biol 54:857–863

Fahey JV, Wright JA, Shen L, Smith JM, Ghosh M, Rossoll RM, Wira CR (2008) Estradiol selectively regulates innate immune function by polarized human uterine epithelial cells in culture. Mucosal Immunol 1:317–325

Franke S, Ruster C, Pester J, Hofmann G, Oelzner P, Wolf G (2011) Advanced glycation end products affect growth and function of osteoblasts. Clin Exp Rheumatol 29:650–660

Giannoni E, Guignard L, Knaup Reymond M, Perreau M, Roth-Kleiner M, Calandra T, Roger T (2011) Estradiol and progesterone strongly

inhibit the innate immune response of mononuclear cells in newborns. Infect Immun 79:2690–2698

Graziano A, d'Aquino R, Laino G, Papaccio G (2008) Dental pulp stem cells: a promising tool for bone regeneration. Stem Cell Rev 4:21–26

Iejima D, Sumita Y, Kagami H, Ando Y, Ueda M (2007) Odontoblast marker gene expression is enhanced by a CC-chemokine family protein MIP-3alpha in human mesenchymal stem cells. Arch Oral Biol 52:924–931

Johnson RB, Gilbert JA, Cooper RC, Dai X, Newton BI, Tracy RR, West WF, DeMoss TL, Myers PJ, Streckfus CF (1997) Alveolar bone loss one year following ovariectomy in sheep. J Periodontol 68:864–871

Kanda N, Watanabe S (2003) 17Beta-estradiol inhibits the production of RANTES in human keratinocytes. J Invest Dermatol 120:420–427

Kawamoto S, Ejiri S, Nagaoka E, Ozawa H (2002) Effects of oestrogen deficiency on osteoclastogenesis in the rat periodontium. Arch Oral Biol 47:67–73

Khosla S, Melton LJ 3rd, Riggs BL (2011) The unitary model for estrogen deficiency and the pathogenesis of osteoporosis: is a revision needed? J Bone Miner Res 26:441–451

Komori T (2010) Regulation of osteoblast differentiation by Runx2. Adv Exp Med Biol 658:43–49

Laino G, d'Aquino R, Graziano A, Lanza V, Carinci F, Naro F, Pirozzi G, Papaccio G (2005) A new population of human adult dental pulp stem cells: a useful source of living autologous fibrous bone tissue (LAB). J Bone Miner Res 20:1394–1402

Lee SS, Sharma AR, Choi BS, Jung JS, Chang JD, Park S, Salvati EA, Purdue EP, Song DK, Nam JS (2012) The effect of TNFalpha secreted from macrophages activated by titanium particles on osteogenic activity regulated by WNT/BMP signaling in osteoprogenitor cells. Biomaterials 33:4251–4263

Ma D, Ma Z, Zhang X, Wang W, Yang Z, Zhang M, Wu G, Lu W, Deng Z, Jin Y (2009) Effect of age and extrinsic microenvironment on the proliferation and osteogenic differentiation of rat dental pulp stem cells in vitro. J Endod 35:1546–1553

Mamalis A, Markopoulou C, Lagou A, Vrotsos I (2011) Oestrogen regulates proliferation, osteoblastic differentiation, collagen synthesis and periostin gene expression in human periodontal ligament cells through oestrogen receptor beta. Arch Oral Biol 56:446–455

Moriya Y, Ito K, Murai S (1998) Effects of experimental osteoporosis on alveolar bone loss in rats. J Oral Sci 40:171–175

Muhammad N, Luke DA, Shuid AN, Mohamed N, Soelaiman IN (2012) Two different isomers of vitamin E prevent bone loss in postmenopausal osteoporosis rat model. Evid Based Complement Alternat Med: eCAM 2012:161527

Ni P, Fu S, Fan M, Guo G, Shi S, Peng J, Luo F, Qian Z (2011) Preparation of poly(ethylene glycol)/polylactide hybrid fibrous scaffolds for bone tissue engineering. Int J Nanomed 6: 3065–3075

Takahashi T (2011) Overexpression of Runx2 and MKP-1 stimulates transdifferentiation of 3T3-L1 preadipocytes into bone-forming osteoblasts in vitro. Calcif Tissue Int 88:336–347

Tang Y, Xie H, Chen J, Geng L, Chen H, Li X, Hou Y, Lu L, Shi S, Zeng X, Sun L (2013) Activated NF-kappaB in bone marrow mesenchymal stem cells from systemic lupus erythematosus patients inhibits osteogenic differentiation through downregulating Smad signaling. Stem Cells Dev 22:668–678

Wade-Gueye NM, Boudiffa M, Vanden-Bossche A, Laroche N, Aubin JE, Vico L, Lafage-Proust MH, Malaval L (2012) Absence of bone sialoprotein (BSP) impairs primary bone formation and resorption: the marrow ablation model under PTH challenge. Bone 50:1064–1073

Wang S, Mu J, Fan Z, Yu Y, Yan M, Lei G, Tang C, Wang Z, Zheng Y, Yu J, Zhang G (2012) Insulin-like growth factor 1 can promote the osteogenic differentiation and osteogenesis of stem cells from apical papilla. Stem Cell Res 8:346–356

Wang YX, Ma ZF, Huo N, Tang L, Han C, Duan YZ, Jin Y (2011) Porcine tooth germ cell conditioned medium can induce odontogenic differentiation of human dental pulp stem cells. J Tissue Eng Regen Med 5:354–362

Wattanaroonwong N, Schoenmaker T, Vries TJ de, Everts V (2011) Oestrogen inhibits osteoclast formation induced by periodontal ligament fibroblasts. Arch Oral Biol 56:212–219

Xu J, Wu HF, Ang ES, Yip K, Woloszyn M, Zheng MH, Tan RX (2009) NF-kappaB modulators in osteolytic bone diseases. Cytokine Growth Factor Rev 20:7–17

Yamaguchi M, Arbiser JL, Weitzmann MN (2011) Honokiol stimulates osteoblastogenesis by suppressing NF-kappaB activation. Int J Mol Med 28:1049–1053

Yan M, Yu Y, Zhang G, Tang C, Yu J (2011) A journey from dental pulp stem cells to a bio-tooth. Stem Cell Rev 7:161–171

Yang X, Zhang S, Pang X, Fan M (2012) Pro-inflammatory cytokines induce odontogenic differentiation of dental pulp-derived stem cells. J Cell Biochem 113:669–677

Yu J, He H, Tang C, Zhang G, Li Y, Wang R, Shi J, Jin Y (2010) Differentiation potential of STRO-1+ dental pulp stem cells changes during cell passaging. BMC Cell Biol 11:32

Yu Y, Mu J, Fan Z, Lei G, Yan M, Wang S, Tang C, Wang Z, Yu J, Zhang G (2012) Insulin-like growth factor 1 enhances the proliferation and osteogenic differentiation of human periodontal ligament stem cells via ERK and JNK MAPK pathways. Histochem Cell Biol 137:513–525

Zhang B, Li Y, Zhou Q, Ding Y (2011a) Estrogen deficiency leads to impaired osteogenic differentiation of periodontal ligament stem cells in rats. Tohoku J Exp Med 223:177–186

Zhang J, Tu Q, Grosschedl R, Kim MS, Griffin T, Drissi H, Yang P, Chen J (2011b) Roles of SATB2 in osteogenic differentiation and bone regeneration. Tissue Eng Part A 17:1767–1776

Zhang M, Chen FM, Wang AH, Chen YJ, Lv X, Wu S, Zhao RN (2012) Estrogen and its receptor enhance mechanobiological effects in compressed bone mesenchymal stem cells. Cells Tissues Organs 195:400–413

Zhao JW, Gao ZL, Mei H, Li YL, Wang Y (2011) Differentiation of human mesenchymal stem cells: the potential mechanism for estrogen-induced preferential osteoblast versus adipocyte differentiation. Am J Med Sci 341:460–468